Islamic Azad University
Mashhad Branch

M. Javanbakht et al. / Iranian Journal of Earth Sciences 3 (2011) / 108 - 118

Depositional History and Sequence Stratigraphy of the Tirgan Formation (Barremian – Aptian) in the Zavin section, NE Iran

M. Javanbakht[1]*, R. Moussavi Harami[2] and A. Mahboubi[2]

1. Department of Geology, Science and Research Branch, Islamic Azad University, Tehran, Iran
2. Department of Geology, Ferdowsi University of Mashhad, Iran
Received 6 February 2011; accepted 7 August 2011

Abstract

The Tirgan Formation (Barremian – Aptian) is exposed in the Kopet Dagh in northeast Iran. One stratigraphic section in Zavin was measured with a thickness of 110 meters. This Formation in section consists of three parts (including lower carbonate, limy shale – marl and upper carbonate rocks). Based on the study of 94 thin sections, 10 carbonate and 2 siliciclastic lithofacies have been identified. Carbonate lithofacies were deposited in a ramp platform in fore-shoal, shoal, lagoon and tidal flat environments. Sea level changes during the early Cretaceous time led to the formation of different large scale depositional sequences Zavin (two). The present data can help in the reconstruction of the tectonic history of the area during early Cretaceous time.

Keywords: *Early Cretaceous, Tirgan Formation, Zavin, Depositional sequence.*

1. Introduction

The Kopet-Dagh sedimentary basin was formed in northeast Iran, southwestern Turkmenistan and north Afghanistan after the closure of the Paleotethys Ocean following the Middle Triassic Orogeny that involved the Iran and Turan plates [1, 2, 3 and 4].The Kopet – Dagh basin formed in an extensional regime during the Early to Middle Jurassic [5]. The Kopet-Dagh orogenic belt is an inverted basin [6]. Over 6000 m of sedimentary rocks ranging in age from Middle Jurassic to Miocene were deposited in the basin [7] and can be assigned to five major transgressive – regressive sequences [8]. Basin subsidence was initiated along major east – west longitudinal faults during the Jurassic period [7, 9 and 10], but Moussavi – Harami and Brenner [8] suggested that much of the post- Jurassic subsidence in the eastern Kopet - Dagh was caused by sediments rather than tectonic loading. Jurassic-Cenozoic carbonates and siliciclastics unconformably overlie the Paleozoic (basement) and Triassic rocks [11]. The Lower Cretaceous carbonates in the Kopet-Dagh basin constitute one of the potential petroleum reservoirs. Lower Cretaceous deposits in the Kopet-Dagh are nominated as the Tirgan Formation. Marine progression in the Barremian – Aptian led to the deposition of the Tirgan Formation. The Lower Cretaceous marine sequence of Tirgan Formation is exposed along the northwest-southeast trending anticlines and synclines in the central and eastern parts of the Kopet-Dagh basin.

---

*Corresponding author.
E-mail address (es): mo_ja@yahoo.com

This formation is composed principally of ooid limestone, sandstones, dolomites in the base and marl – shale in the top, and crops out along the Kopet-Dagh Range. The Tirgan Formation is conformably overlain by marl – shale of the Sarcheshmeh Formation and is conformably underlain by the siliciclastic red beds of the Shourijeh Formation.

In order to study the Tirgan Formation, 1 section in the central Kopet-Dagh was surveyed (Fig.1). The thickness of this section is 110m and it consists of three parts: lower carbonate, limy shale – marl and upper carbonate rocks (Fig.2). The objectives of this study were to analyze the facies, to interpret the depositional environment, to delineate the sequence of the stratigraphic units and boundaries and to determine the processes responsible for the development of sequences in central Iran.

2. Methods of Study

This study is based on 94 thin sections that were stained using Alizarin red S [12] and studied using standard petrographic microscopic techniques. Carbonate rocks were classified according to Dunham's carbonate classification [13] and Embry and Kloven [14]. Siliciclastic rocks were classified using Folk's classification [15]. In petrographic studies the major and minor allochems were recognized and the Clasticity Index (CI) was determined. In order to delineate CI, ooid, intraclast, echinoid and quartz diameters were measured. The CI was used for the interpretation of environment energy. Field and petrographic studies were carried out to describe the microfacies to interpret the depositional environments.

Sequence stratigraphy of the Lower Cretaceous interval was interpreted by analyzing the facies based on the methods proposed by Wilson [16], Flugel [17] and Carozzi [18]. Sequence stratigraphic techniques and concepts developed by many workers were used in this study to delineate sequence boundaries (unconformities) and parasequences based on marine flooding surfaces [19, 20, 21, 22, 23 and 24]. Finally sea level curves in the studied area were compared with the sea level curve on the global scale [19].

3. Lithofacies Description and Interpretation

The strata of the Tirgan Formation are subdivided into 10 carbonate and 2 siliciclastic lithofacies. Carbonate lithofacies were recognized along 4 carbonate belts: tidal flat, lagoon, shoal and open marine. Siliciclastic lithofacies were recognized in two classes: sandstones and shaly facies. To facilitate the naming of facies, the minimum amount of allochems was considered as 25%.

Tidal Flat Belt:

Laminated Algal Stromatolite (A1)

The laminated algal stromatolite facies consists of an algal boundstone that has significant amounts of pellets of algal fragments. In thin section, this lithology consists of alternating light and dark gray pelletoidal micritic laminae that have scattered filaments of molds of algae, or cyanobacteria, and of lighter laminae of micrite (Fig. 3a). Along the outcrop belt, this facies is characterized by irregular to regular thinly laminated strata, which are gray and light in color (Fig. 3b).

Mudstone - Dolomudstone (A2)

This facies contains limy mud and it is low in bioclasts (Fig. 3c). Partial dolomitization and fenestral fabric were observed. In outcrop, this facies is thin to medium-bedded and dark gray in color. It shows fenestral fabric and lamination.

Ooid Grainstone (A3)

The ooid grainstone facies contains ooids (60-65%), bivalves, brachiopods, bryozoans and echinoderms. Bioclast sizes range between (1.2-1.4mm). In addition, this facies contains pellets and intraclasts (Fig. 3e) which range in size from 0.5mm to more than 2 mm in some thin sections. Also in some thin sections, there are about 7-8% silt sized siliciclastic grains. Along the outcrop belt, this facies is gray medium- bedded and shows cross-bedding.

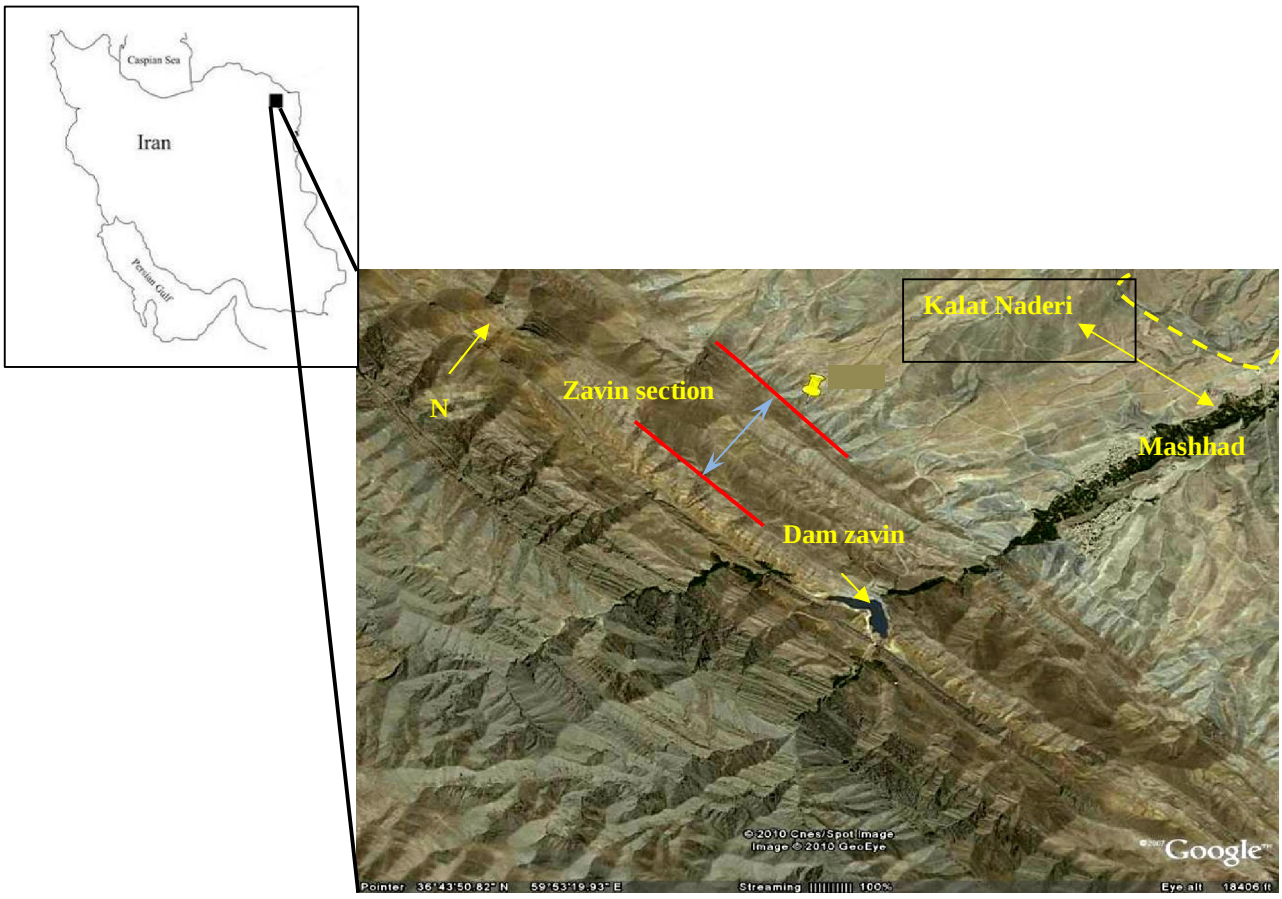

Fig. 1. Location Map of the Tirgan formation in the Zavin sections.

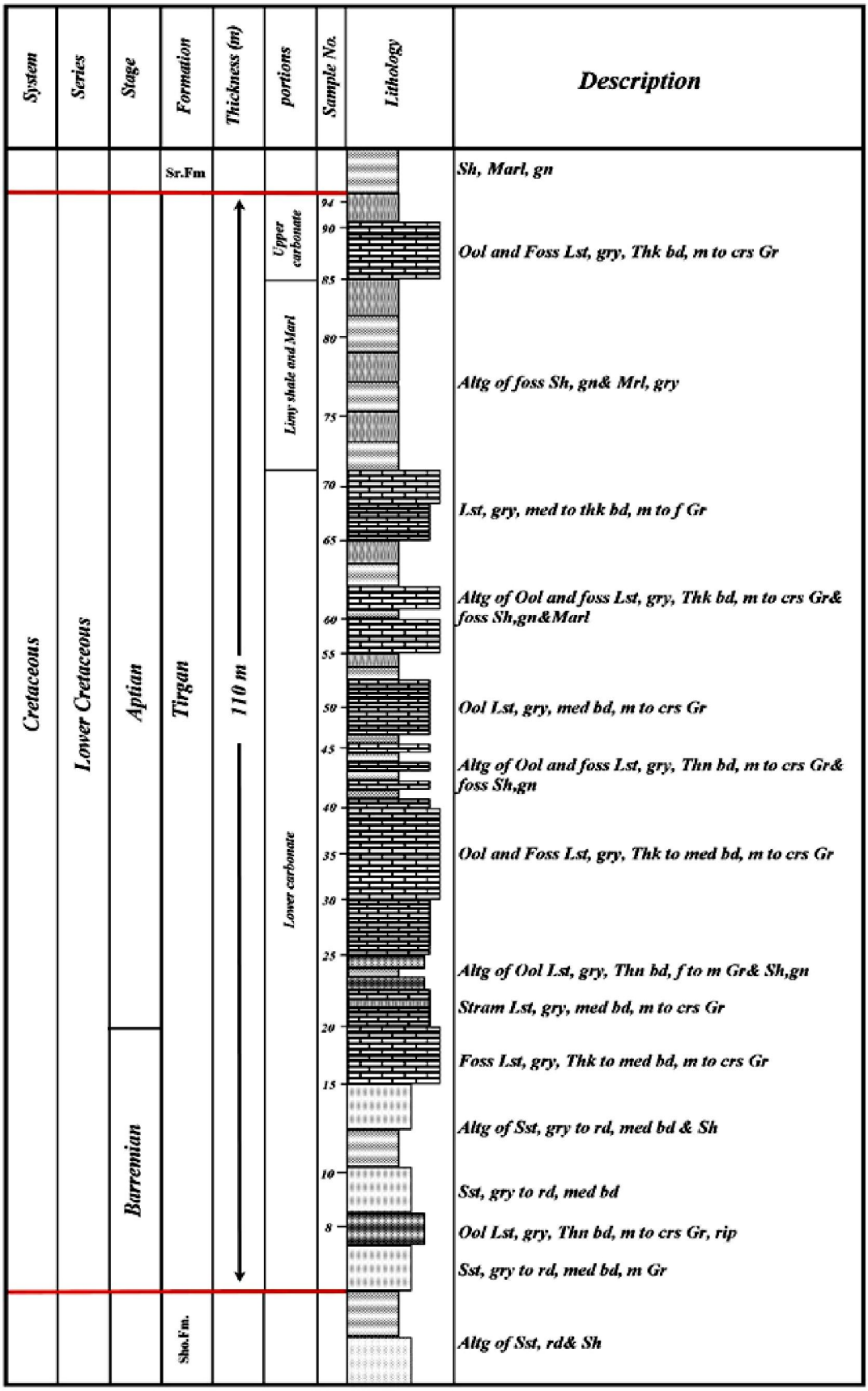

Fig. 2. Stratigraphy of the Tirgan Formation: Zavin Section

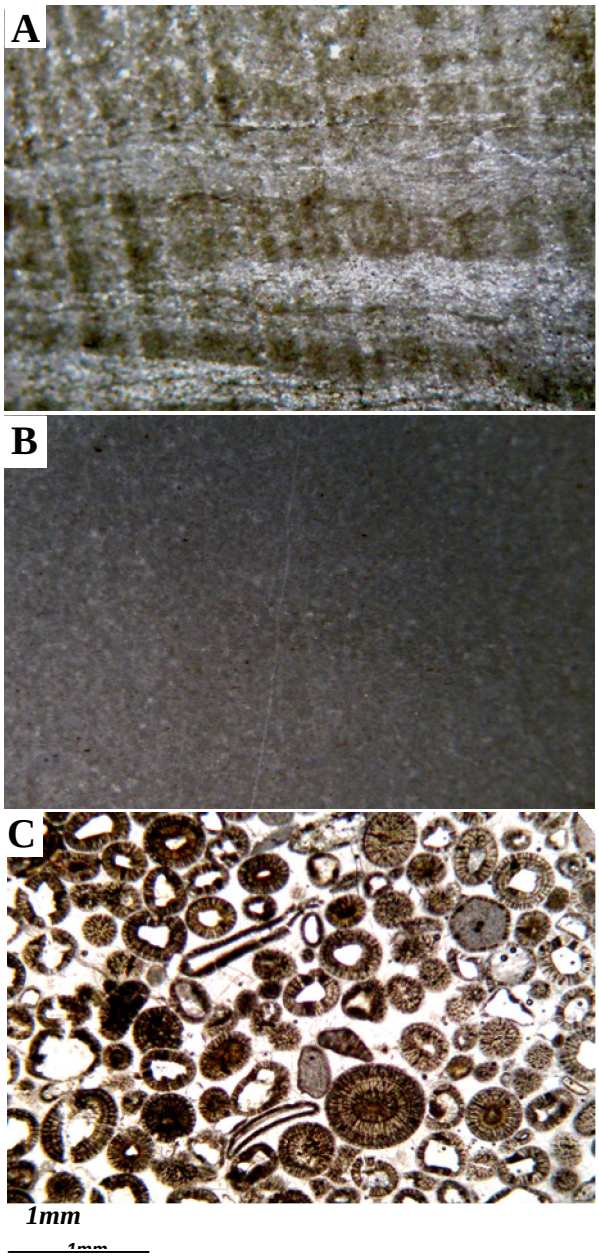

Fig.3. Intertidal Facies of the Tirgan Formation A: Laminated algal stromatolite B: Mudstone C: Ooid Grainstone.

Lagoon Belt (B)

Ooid Packstone – Wackestone (B1)

Ooid Packstone – Wackestone facies consists of 12% wackestone and 45% packstone. In the Packstone facies, there are lesser amounts of bioclasts (20%) including bryozoans, brachiopods, green alga, gastropods and pellets (8-10%) (Fig.4a). The size of ooids varies between 1-1.2mm. Ooids are mostly with cortex and radial fabric. In some thin section, ooids were micritized. Along the outcrop belt, this subfacies is characterized by thin to medium- bedding, dark gray color and cross lamination.

Bioclast Packstone – Wackestone (B2)

Bioclast Packstone – Wackestone facies contains skeletal grains (25-50%), pellets (10-12%) and ooids (8-10%) (Fig. 4b). Skeletal grains include Orbitolina (13-15%), bivalve (5-6%), brachiopods (3-5%) and gastropods (3-4%). These strata are thick- bedded, have a gray color and contain large skeletal crusts.

Shoal Belt (C)

Ooid Grainstone (C1)

The Ooid Grainstone facies consists of about 65% ooids. Its clasticity index is 1.5 mm (Fig. 4c). Their fabric is radial and cortex. There is less abundance of skeletal grains (13%) and intraclasts (15%). On the outcrop belt, the facies is thick, gray in color and contains trough and cross bedding.

Bioclast Grainstone (C2)

This facies consists of about 48-53% bioclasts. Most skeletal grains range between 1.5 to 2mm and include18-20% brachiopods (1.5-2mm), 15-18% bivalves (1.5mm) and 15%Orbitolina (1-1.2mm) (Fig. 4d). There is an abundance of non-skeletal grains consisting of intraclasts (15%) and ooids (5%). On the outcrop belt, the facies is medium-bedded, gray in color and shows cross- bedding.

Fore Shoal Belt (D)

Ooid Packstone (D1)

This facies was observed in the upper part of formation. It consists of ooids (max 55%), bivalves, Orbitolina, brachiopods, oncoids and intraclasts. Clasticity index of ooids is 1 mm and for intraclasts it is 2.5 mm (Fig. 5a). In some thin sections the abundance of intraclasts is 15%. Along the outcrop belt, these gray strata are medium to thick- bedded.

Bioclast Packstone – Wackestone (D2)

This facies consist of Orbitolina (15-16 %) ranging in diameter from 1-1.7 mm, brachiopods (10-12 %) ranging in diameter from 0.7 mm, and bivalves (8-10 %) ranging in diameter from 0.8 mm. Moreover, oncoids account for 12-15% and range in diameter from 2-2.5mm (Fig. 5b). In outcrop, this facies is thick-bedded, gray in color and contains lamination.

Bioclast Mudstone – Mudstone (D3)

This facies includes Orbitolina (5-6%) ranging in diameter from 0.6-0.7 mm, bivalves (3-4%) ranging in diameter from 0.4-0.5 mm and brachiopods (2%) ranging in diameter from 0.4 mm (Fig. 5c). Along the out crop belt, this facies is thin to medium- bedded and dark gray in color.

Siliciclastic Belt

Sandstone facies (S)

This facies was located in the lower part of the section. The sandstone facies consist of subarkose to sublitharenite. The subarkose consists of quartz (80-85%), feldspar (11%) and lithics (2-3%). Most of the feldspars are plagioclase. Sub-litharenite consists of

lithics (10-12%) and feldspar (2%). Most lithic grains are chert and the feldspar is plagioclase (Fig. 6a, b) This facies contains both horizontal and cross-bedded strata sets and the grain size ranges from fine to medium- grained sandstones. This facies is mature; outcrop colors range from gray to red. This facies includes carbonate and silica cement.

Shale Facies (SH)

This facies can be divided into two subfacies. The first subfacies consist of red to green shale that is thinly laminated and has a low abundance of fossils. This facies is located in the lower part of the sections (Fig. 7a). This subfacies is divided into two classes. The first class is related to the sandstones and the tidal belt carbonate facies (Sh1) and the second class is related to the lagoon belt carbonate facies (Sh2). The second subfacies is characterized by thinly laminated gray to green calcareous shale (Sh3), containing echinoderms and Orbitolina that is related to shoal and fore-shoal belt (Fig. 7b). This subfacies is located in the upper part of the section.

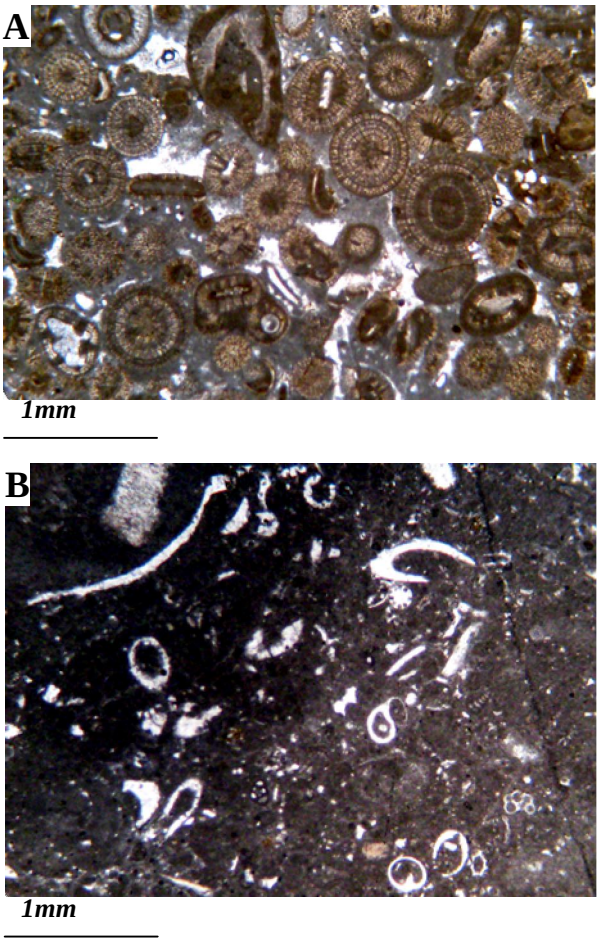

Fig. 4. Lagoon Facies of the Tirgan Formation A: Ooid Packstone- Wackstone B: Bioclast Packstone- Wackstone.

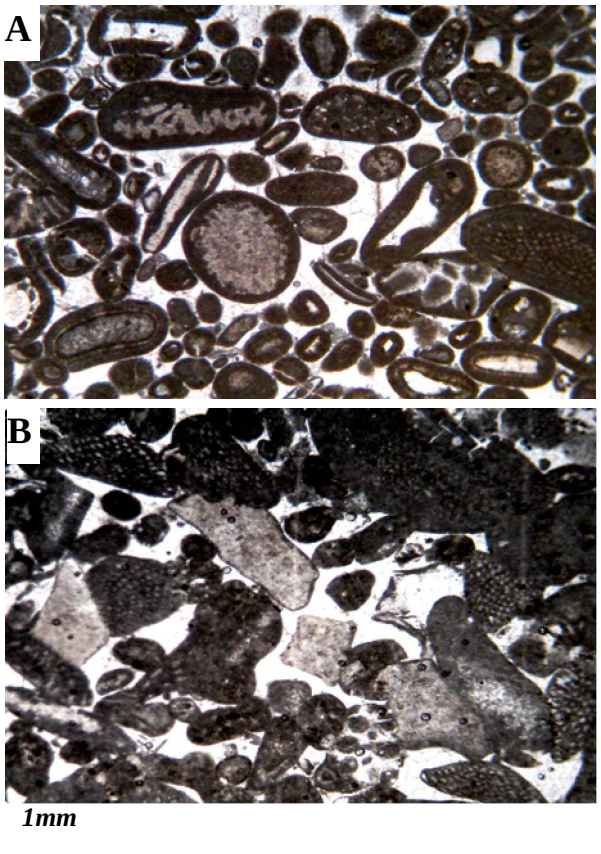

Fig. 5. Shoal facies of the Tirgan Formation A: Ooid Grainstone B: Bioclast Grainstone.

4. Interpretation and Modeling of depositional environments

In the Stromatolite and Mudstone facies, according to the low abundance of fossils and the fine-grained sediments, a low energy supratidal environment is deduced [25, 26]. Lack of fossils in this facies, shows a water cycle limit and unsuitable marine organism conditions [27,28]. Good sorting of ooid grainstone facies, the high clasticity index of most of the facies and the carbonate mud show high energy environment. Muddy intraclasts and high abundance of pelloids close to the lagoon indicate tidal environments [29].

Allochems in the Bgroup facies such as pellets, ostracoda, green alga, miliolidae, gastropods, Orbitolina and higher abundance of mud show deposition in a low energy environment [30].Ooid and fecal pellets indicate such an environment, too [31, 32]. Coarse muddy intraclasts in the Packstone facies show deposition in a high energy lagoon and proximity to shoal [33].

Abundance of skeletal grains such as miliolidae and gastropods usually indicate back reef lagoons [34]. In addition, there are high abundances of pellets in low-energy water, warm, high calcite saturation and lagoon in the back of the barrier [33, 35].

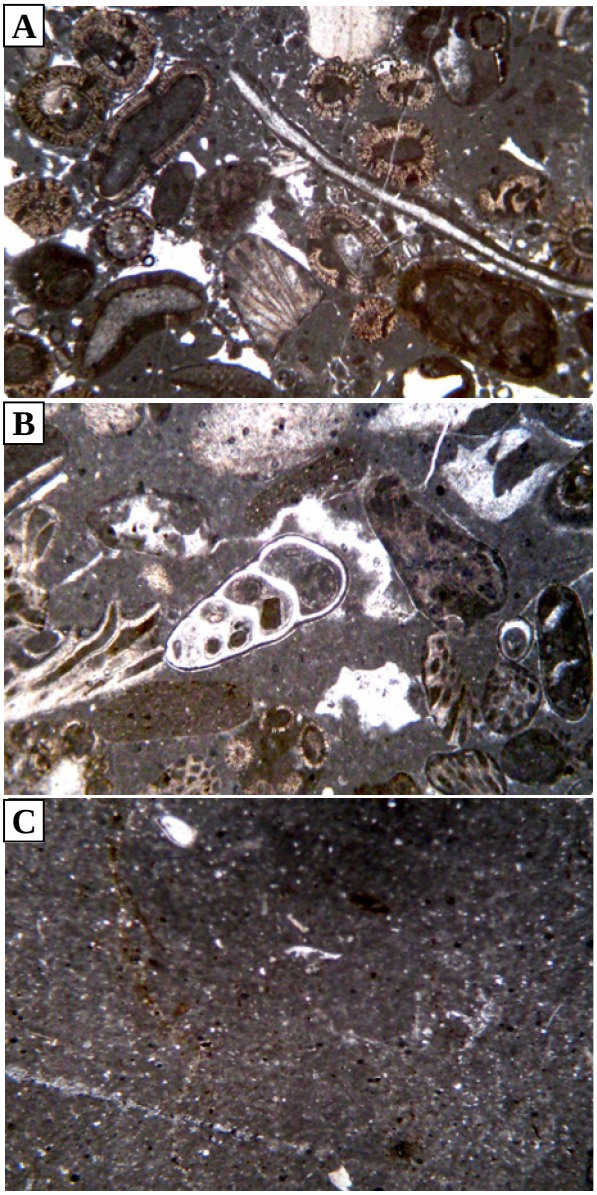

Fig. 6. Fore Shoal facies of the Tirgan Formation A: Ooid Packstone B: Bioclast Wackstone- Packstone C: Mudstone – Bioclast Mudstone.

Less abundance of stenohalina such as echinoderms and brachiopods show that the lagoon was connected to the open sea.

Grain supported ooid grainstones without any mud indicate deposition in a high energy belt [17, 36]. Ooid grainstones occur in high temperature, shallow wavy water (less than 2 m), with a normal salinity [29, 37] while intraclasts and stenohalina indicate a barrier environment [17].

Moreover, the skeletal grains such as echinoderm, bivalves, brachiopods and less abundant Orbitolina (abundance of Orbitolina increases in the upper part of the section) resembles some skeletal grains of an open sea where echinoderm and brachiopods indicate deposition between lagoon and open marine environments [38].

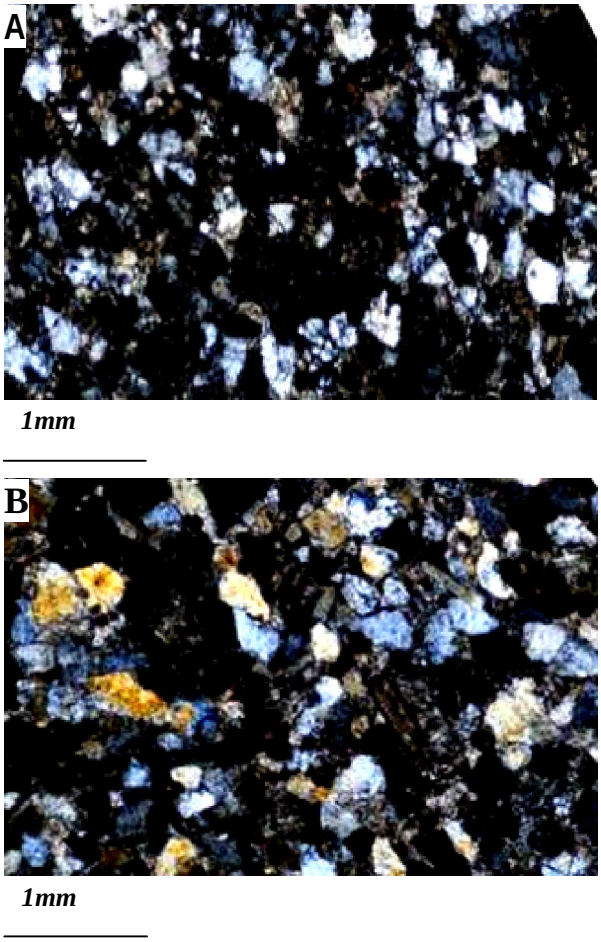

Fig. 7. Sandstone facies of the Tirgan Formation A: sub-arkose B: sub-litharenite.

Skeletal grains in the D facies group consist of Orbitolina, brachiopods, bivalves, echinoderm and bryozoans. These are sensitive to salinity and an open marine environment is suitable for their life [17, 39, and 40]. According to the abundance of stenohalina, high abundance of mud and thin-bedded layers, we can consider a low energy environment and low sedimentation for this facies which indicates open marine environment [17, 41]. Minor amounts of non-skeletal grains such as ooids and intraclasts in this facies were moved from adjacent high energy environments. In this facies, close to the barrier, the amount of limy mud was decreased, and the abundance of allochems increased that indicates an increase in energy and proximity to barrier environments [40].

Well-sorted, well-rounded grains and the absence of matrix show formation of mature sandstone which indicates beach-type depositional setting. Also low-angle stratification and skeletal grains indicate a beach setting for the siliciclastic facies [42].

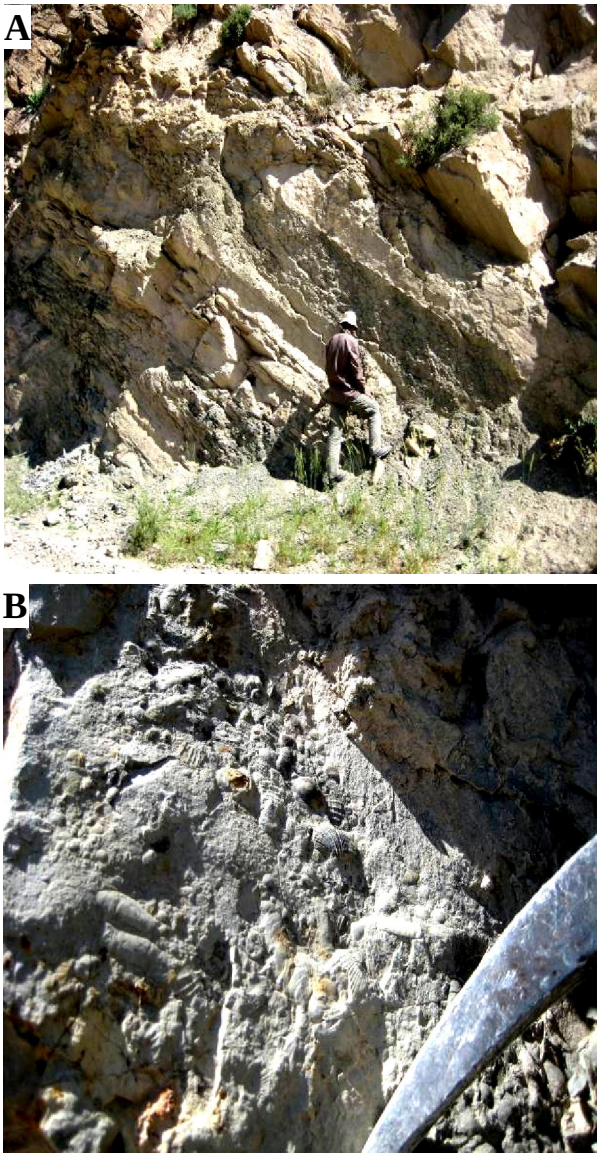

Fig. 8. Shaly facies of the Tirgan Formation A: Shale without fossils at the base B: Upper shale with macrofossils.

Based on the facies description, recent studies [43] and comparison to already presented models [17, 44 and 45] a depositional model of the Tirgan Formation was constructed for the studied area. Therefore according to the facies type and vertical changes in the studied section and based on the gradual changes of Tirgan Formation from the Shourijeh Siliciclastic Formation to the Sarcheshmeh Marine Shale, the environment of this formation is considered as a carbonate ramp-type platform [46, 47](Fig.8).

5. Sequence stratigraphy

Deposition of the Tirgan supersequence (Baremian – Aptian) occurred in about 10 million years [7, 48 and 49]. The deposition time of the constituent parasequences was estimated based on their thickness and comparing them with the formation's thickness. This estimation excludes parameters like variations of depositing rate, compaction, tectonic and other factors, while conditions for the entire formation were considered to be the same. Each sequence was explained in this paper in the proper section.

Sedimentary Sequences in the Zavin Section

In this section two sedimentary sequences were identified which form some sedimentary parasequences (Fig. 9).

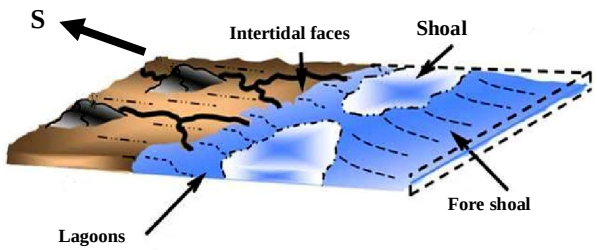

Fig. 9. Sedimentary model of the Tirgan Formation in the Zavin section

Sedimentary sequence 1

Lower and upper boundaries of this sequence are type 2 (SB2) [24, 50, 51, and 52]. In the Van Wagnor approach [20] this boundary indicates fall in sea level without changes in shoreline location.

The thickness of this sequence is about 35.5 meters. The base of TST is characterized by the Dolomudstone facies. In most of the facies, dolomitization is observed which could happen in TST level [30]. In this sequence TST deposits were formed comprising some lithofacies which show transgressive relations. This transgressive system tract includes sediments from intertidal (mudstone, ooid grainstone and sandstone) to lagoon (ooid packstone - wackestone and bioclast packstone - wackestone) environment.

The Bioclast Wackestone facies shows maximum flooding surface of this sequence. The TST deposits formed consist of two deepening upward parasequences. According to the thickness of this part (30m) and its age, this section appears to have been deposited in 1.26 million years. The HST system tract included tidal flat and lagoon sediments. This system tract contains one shallowing upward parasequence. The upper boundary of this sequence is characterized by intertidal stromatolite which indicates falling sea level and is considered as a SB2 type. This sequence has 5.23 meters thickness and was deposited during 0.47 million years.

Sedimentary Sequence 2

This sequence is characterized by SB2 at the base and the top. This sequence is the main part of the Zavin Section.

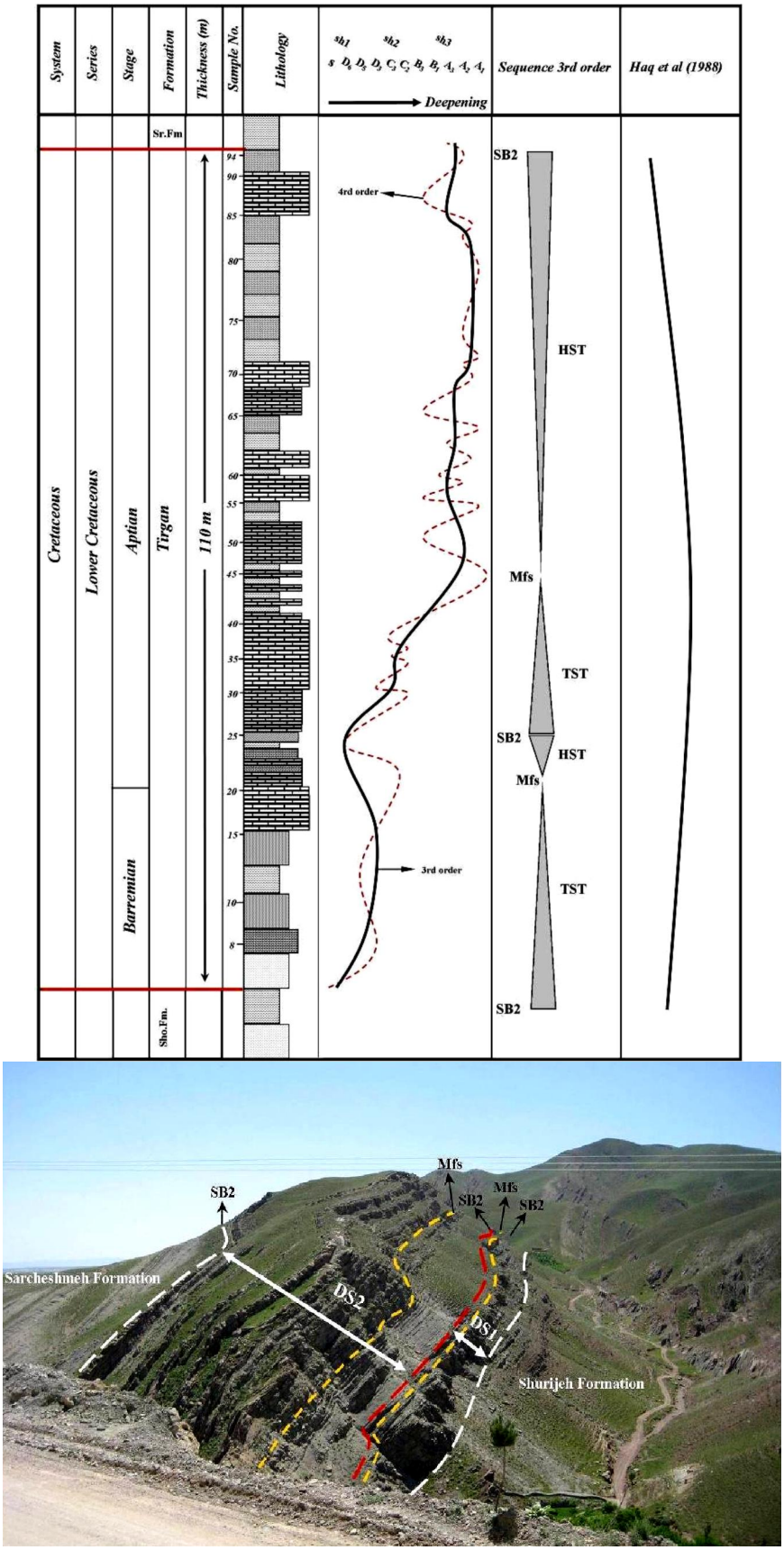

Fig. 10. Facies changes and sedimentary sequences of the Tirgan Formation in the Zavin Section.

This sequence has a thickness of 74.5 meters and it was deposited during 6.7 million years.

The TST of sedimentary sequence 2 includes intertidal, lagoon, barrier and open marine facies which are 21 meters in thickness and form four deepening upward parasequences.

The deposition of Mudstone facies related to open marine conditions indicates the maximum flooding surface. Above this surface the HST is characterized by open marine and shoal facies which include nine shallowing upward parasequences. The upper sequence boundary is located in the Sarcheshmeh Formation which is SB2 type. This sequence has a thickness of 53 meters and was deposited during 4.8 million years.

6. Sea Level Changes Interpretation

After identifying the sedimentary sequences in the Zavin Section, the sea level changes curve was compared with the global sea level changes curve during Barremian – Aptian time which has been presented by Haq et al. [19].

The same mega cycle (ZUNI) in Barremian – Aptian shows rising sea levels that confirm changes of Shourijeh siliciclastic facies to Tirgan carbonate and Sarcheshmeh marine shale.

The Tirgan supersequence is mainly coincident with the global super cycle (ZUNI II-1) where the main differences are in its sequences; the Tirgan formation has two sequences while the global sea level curve has one 3rd class sedimentary sequence. The differences between the sedimentary sequence (third class) and the observed parasequence (4th and 5th class) in the studied sections when compared to the global sea level curves are because of tectonic parameters that changed the environmental conditions during sedimentation and formation of different sedimentary facies [53, 54, 55, 56, 57 and 58].

7. Conclusions

The early Cretaceous deposits of the Tirgan formation in the Kopet Dagh Basin (Zavin section) are composed of four carbonate lithofacies belts containing 10 facies and two siliciclastic lithofacies. These facies formed in a sub-environment that consisted of fore-shoal (the Bioclast Mudstone – Mudstone, the Bioclast Packstone – Wackestone and the Ooid Packstone), grain – rich shoal (the Bioclast Grainstone and the Ooid Grainstone), semi-restricted lagoon (the Bioclast Packstone – Wackestone and the Ooid Packstone – Wackestone) and tidal flat (the Ooid Grainstone, the Mudstone and Dolomudstone and the Laminated Algal Stromatolite) deposits, respectively. Some thick intervals of calcareous shale and fine-to medium-grained sandstone are also present interspersed within these carbonate lithofacies.

The lithofacies of the Tirgan formation were deposited in a ramp platform. The Tirgan supersequence is divided into two third class sedimentary sequences with type 2 sequence boundaries.

References

[1] Berberian, M. and King, G.C.P., 1981, Toward a paleogeography and tectonic evolution of Iran: Canadian Journal of Earth sciences, v.18, p.210-265.

[2] Rüttner, A. W., 1991, Geology of the Aghdarband area (Kopet Dagh NE Iran), Abhandlungen der Geologischen Bundesanstalt, v.38, p.7-79

[3] Alavi, M., Vaziri, H., Seyed-Emami, K. and Lasemi, Y., 1997, The Triassic and associated rocks of the Aghdarband areas in Central and north eastern Iran as remnants of the southern Turanian active continental margin, Geological Society of America Bulletin, v.109, p.1563-1575.

[4] Buryakovsky, L. A., Chilinger, G. V. and Aminzadeh, F., 2001, Petroleum Geology of South Caspian Basin, Gulf Professional Publishing, USA, 422pp.

[5] Garzanti, E. and Gaetani, M., 2002, Unroofing history of Late Paleozoic magmatic arcs within the "Turan Plate" (Turkmenistan)", Sedimentary Geology, v.151, p.67-87

[6] Allen, B., Vincent, S. T., Alsop, G. I., Ismail-Zadeh, A., and Fleckerd, R., 2003, Late Cenozoic deformation in the south Caspian Region; Effect of rigid basement block within a collision zone. Tectonophysics, v.366, p.223-239

[7] Afshar-Harb, A., 1979, The stratigraphy, Tectonics and petroleum Geology of the Kopet-Dagh Region, Northern Iran, Ph.D. Thesis, Imperial College of Sciences, University of London, United Kingdom, 316pp.

[8] Moussavi-Harami, R., and Brenner, R.L., 1992, Geohistory analysis and petroleum reservoir characteristics of Lower Cretaceous (Neocomian) sandstone, eastern portion of Kopet-Dagh basin, northeast Iran, A.A.P.G Bulliten, v. 76, p. 1200-1208.

[9] Afshar-Harb, A., 1982a, Geological Map of Sarakhs Area, National Iranian Oil Company, Geological division, Exploration and Production, Scale 1:250000, 1 sheet.

[10] Afshar-Harb, A., 1982b, Geological Map of Daregaz Area, National Iranian Oil Company, Geological division, Exploration and Production, Scale 1:250000, 1 sheet.

[11] Ulmishek, G., 2004, Petroleum Geology and resource of the Amo-Darya basin, Turkmenistan, Uzbekistan, Afghanistan and Iran. USGS Bull., p. 2201-4, 32pp

[12] Dickson, J.A.D., 1966, Carbonate identification and genesis as revealed by staining, Journal of Sedimentary Petrology, v.36, p.491-505.

[13] Dunham, R.J., 1962, Classification of carbonate rocks according to depositional texture", In W.E. Ham (Editor), Classification of Carbonate Rocks-A Symposium, American Association of Petroleum Geologists, Memoir 1, p.108-121.

[14] Embry, A.F. and Kloven, J.E., 1971, A Late Devonian reef tract on northeastern Banks Island, Northwest Territories, Bulletin Canadian Petroleum Geology, v.19, p. 730-781.

[15] Folk, R.L., 1980, Petrology of Sedimentary Rocks: Hemphill Publishing Co. Austin, Texas, 182pp.
[16] Wilson, J.L., 1975, Carbonate Facies in Geologic History, Springer-Verlag, 471pp.
[17] Flugel, E., 2010, Microfacies Analysis of Carbonate Rocks: Analysis, Interpretation and Application, 2nd edition, Springer-Verlag, 984pp.
[18] Carozzi, A.V., 1989, Carbonate Rocks Depositional Models: A Microfacies Approach, Prentice-Hall, 604pp.
[19] Haq .B.U., Hrdenbol, J., and Vial, P.R., 1988, Mesozoic and Cenozoic chronostratigraphy and eustatic cycles, in P.D. Grevello, J.L. Wilson, J.F. Sarge. And J.F. Read (Editors), Controls on carbonate platform and basin development, SEPM Special Publication, v.44, p.71-108
[20] Van Wagoner, J.C., Mitchum, R.M., Campion, K.M. and Rahmanian, V.D., 1990, Siliciclastic Sequence Stratigraphy in Well Logs, Core, and Outcrops: Concepts for High-Resolution Correlation of Time and Facies, AAPG Methods, in Exploration Series No. 7, The American Association of Petroleum Geologists, Tulsa OK, 55 pp.
[21] Sarg, L.F., 1988, Carbonate sequence stratigraphy, In: C.K. Wilgus, B. S. Hastings, C.G.St.C. Kendall, H. W. Posamnetier, C.A. Ross and J.C. Van Wagoner (editors), Sea Level Changes: An Integrated Approach, Society of Economic Paleontologists and Mineralogists, Special Publication, v. 42, p.155-181.
[22] Handford, C.R., and Loucks, R.G., 1993, Carbonate depositional sequences and System Tracts-responses of carbonate platforms to relative sea level change, In: R.G. Loucks and J.F. Sarg (editors), Carbonate Sequence Stratigraphy: Recent Developments and Applications, American Association of Petroleum Geologists, Memoir v.57, p.3-41.
[23] Read, J.F., 1998, Phanerozoic carbonate ramps from greenhouse, transitional and ice-house worlds: clues from field and modeling studies, Geological Society, London, Special Publications, v. 149, p.107-135.
[24] Emery, D. and Myers, K., 1996, Sequence Stratigraphy, Blackwells, Oxford, 297pp.
[25] Preto, N., and Hinnov, L.A., 2003, Unravelling the origin of carbonate platform cyclothems in the Upper Triassic, Durrenstein formation (Dolomite, Italy), Journal of Sedimentary Research, v.73, p.774-789
[26] Nader, F.H., Abdel – Rahman, A. F. M., Haider, A. T., 2006, Petrographic and Chemical traits of Cenomanian Platform Carbonates (center Lebanon): Implications for depositional environments, Cretaceous Research, v.27, p. 689-706.
[27] Warren, J.K., 2006, Evaporites: Sediments, Resources and Hydrocarbons: Springer – Verlag, Berlin, 1035 pp.
[28] Alsharhan, A.S., And Kendall, C.G.ST.C., 2003, Holocene coastal carbonates and evaporites of the southern Arabian Gulf and their ancient analogues: Earth Science Review, v.61, p. 191-243.
[29] Tucker, M.E., 2001, Sedimentary Petrology (3rd edition), Blackwell, Oxford, 262pp.
[30] Tucker, M.E., 1993, Carbonate diagenesis and sequence stratigraphy, In: V.P. Wright (editor), Sedimentology Review, Blackwells, Oxford, p.51-72
[31] Samanckassou, E, Tresch, J., and Strasser, A., 2005, Origin of Peloids in Early Cretaceous deposits, Dorest, South England, Facies., v.51, p. 264-273.
[32] Palma, R., López-Gómez, J. and Piethé, R., 2007, Oxfordian ramp system (La Manga Formation) in the Bardas Blancas area (Mendoza Province) Neuquén Basin, Argentina: Facies and depositional sequences, Sedimentary Geology, v.195, p. 113–134
[33] Adachi, N., Ezaki, Y. and Liu, J., 2004, The fabrics and origins of peloids immediately after the end-Permian extinction, Guizhou Province, South China: Sedimentary Geology, v. 164, p. 161-178.
[34] Wisler, L., Funk, H., and Weissert, H. 2003, Response to Early Cretaceous carbonate platform to change in atmospheric carbonate dioxide level, Palaeogeography, Palaeoclimatology. Palaeoecology, v.200, p. 187-205.
[35] Burchette, T.P. and Wright, V.P., 1992, Carbonate ramp depositional systems, Sedimentary Geology, v.79, p.3-35.
[36] Hafmann, A., Dirks, P.H.G.M., and Jelsma, H.A., 2004, Shallowing upward carbonate cycles in the Blingwe Greenston belt, Zimbabwe: A record of Archean sea level oscillations, J.Sedimentary Research, v.74, no.1, p. 64-81.
[37] Betzler, C., Pawellek, T., Abdullah, M. and Kossler, A., 2007, Facies and stratigraphic architecture of the Korallenoolith Formation in North Germany (Lauensteiner Pass, Ith Mountains), Sedimentary Geology v.194, p.61–75.
[38] Immenhauser, A., Schlager, W., Burns, S. J., Scott, R.W., Geel, T., Lehmann, J., Van der Gaast, S. and Bolder- Schrijwer, L.J.A., 1999, Late Aptian to Late Albian sea-level fluctuations constrained by geochemical and biological evidence (Nahr Umr Formation, Oman), Journal of Sedimentary Research, v.69, p. 434–466.
[39] Tucker, M.E. and Wright, V.P., 1990, Carbonate Sedimentology, Blackwell, Oxford, 482pp.
[40] Sanders, D., and Hofling, R., 2000, Carbonate deposition in mixed siliciclastic-carbonate environments on top of an orogenic wedge (Late Cretaceous, Northern Calcareous Alps, Austria), Sedimentary Geology, v.137, 127-146.
[41] Martini, R., Cirilli, S., Saurer, C., Abate, B., Ferruzza, G., and Cicero, G.L., 2007, Depositional environment and biofacies characterization of the Triassic (Carnian to Rhaetian) carbonate succession of Punta Bassano (Marettimo Island, Sicily), Facies. v. 53 , pp. 389-400.
[42] Nicholas, G., 2000, Sedimentology and stratigraphy, Blackwell Science Ltd, 355pp.
[43] Saffar, A., Mousavi, M. J., Torshizian, H. A., Javanbakht, M., 2010, The Investigation of sedimental Facies and sedimental environment of Tirgan Formation, Zavin Section, NW of Iran, Proceedings of The First International Applied Geological Congress.v.2. p. 2045-2049.
[44] Read, J.F., 1985, Carbonate platform facies models, AAPG Bull., v.69, p.1-21.
[45] Einsele, G., 2000, Sedimentary Basin: Evolution, Facies, and Sediment Budget (2nd edition), Springer-Verlag, 292pp.
[46] Bachman, M., Hirsch, F., 2006, Lower cretaceous carbonate platform of eastern Levant (Galilee and the Golan Heights): stratigraphy and second-order sea level change, Cretaceous Research, v. 27, p. 487-512.
[47] Dobrzinski, N. and Bahlburg, H., 2007, Sedimentology and environmental significance of the Cryogenian successions of the Yangtze platform, South China block,

Palaeogeography, Palaeoclimatology, Palaeoecology, v.254, (1-2), p. 100-122.
[48] Taherpour Khali Abad, M., Schlagintweit, F., Ashouri, A., Aryaei, A. A., 2009, *Juraella bifurcata* BERNIER, 1984 (Calcareous alga, Gymnocodiaceae?) from the Lower Cretaceous (Barremian) Tirgan Formation of the Kopet Dagh basin, north-east Iran, Journal of Alpine Geology, v. 51, p. 79-86.
[49] Taherpour Khali Abad, M., Conrad, M. A., Aryaei, A. A., Ashouri, A., 2010, Barremian-Aptian Dasycladalean algae, new and revisited, from the Tirgan Formation in the Kopet Dagh, NE Iran, Carnets de Géologie / Notebooks on Geology - Article 2010/05 (CG2010_A05).
[50] Al-Husseini, M., 1997, Jurassic sequence stratigraphy of the western and southern Arabian Gulf, GeoArabia, v.2, p.361-382.
[51] Coffey, B.P. and Read, J.F., 2004, Mixed carbonate–siliciclastic sequence stratigraphy of a Paleogene transition zone continental shelf, southeastern USA, Sedimentary Geology, v.166, p.21-57.
[52] Catuneanu, O, 2006, Principles of Sequence Stratigraphy, Elsevier, Amsterdam, 375pp.
[53] El-Azabi, M.H. and El-Araby, A., 2005, Depositional facies, environments and sequence stratigraphic interpretation of the Middle Triassic–Lower Cretaceous (pre-Late Albian) succession in Arif El-Naga anticline, northeast Sinai, Egypt, Journal of African Earth Sciences, v.41, (1-2), p.119-143.
[54] Zecchin, M., 2005, Relationships between fault-controlled subsidence and preservation of shallow-marine small-scale cycles: example from the lower Pliocene of the Crotone Basin (southern Italy), Journal of Sedimentary Research, v.75, p. 300–312.
[55] Zecchin, M., 2007, the architectural variability of small-scale cycles in shelf and ramp clastic systems: The controlling factors, Earth-Science Reviews, v.84, p.21–55.
[56] Zecchin, M., Mellere, D., Roda, C., 2006, Sequence stratigraphy and architectural variability in growth fault-bounded basin fills: a review of Plio–Pleistocene stratal units of the Crotone Basin, southern Italy, Journal of the Geological Society., London v.163, p.471–486.
[57] Rosas, S., Fontboté, L., and Tankard, A., 2007, Tectonic evolution and paleogeography of the Mesozoic Pucará Basin, central Peru, Journal of South American Earth Sciences, v.24, (1), p.1-24
[58] Carpentier, C., Lathuilière, B., Ferry, S., and Sausse, J., 2007, Sequence stratigraphy and tectono-sedimentary history of the Upper Jurassic of the Eastern Paris Basin (Lower and Middle Oxfordian, Northeastern France), Sedimentary Geology, v. 197(3-4), p.235-266.